REVISTA MATÉRIA V.30
ISSN 1517-7076 articlese20250465, 2025

Predictive experimental and mathematical insights into integrating nano-additives and basalt fibre in high-strength concrete beams

Ananthakumar Ayyadurai[1], Saravanan Marudai Muthuchamy[1], Mathiarasu Dhanasekaran[1], Easwaran Paramasivam[2]

[1]Vivekanandha College of Engineering for Women, Department of Civil Engineering. Tiruchengode, 637205, Namakkal, Tamilnadu, India.

[2]Vivekanandha College of Technology for Women, Department of Civil Engineering, Tiruchengode, 637205, Namakkal, Tamilnadu, India.

e-mail: ananthaakumar7410@gmail.com, saromms@gmail.com, mathiarasu65@gmail.com, ereaswarance06@gmail.com

ABSTRACT

This study examines the influence of incorporating Municipal Solid Waste Incineration Ash (MSWIA), nano Municipal Solid Waste Incineration Ash (nMSWIA), Rice Husk Ash (RHA), and nano Rice Husk Ash (nRHA), both with and without basalt fibre, on the development of High Strength Reinforced Concrete Beams (HSRCB). The research explored the mix proportions for ash replacement levels of 5%, 10%, 15%, 20%, 25%, and 30% for each type of ash, alongside the impact of adding 0.5% basalt fibre. A Scanning Electron Microscope (SEM) analysis was conducted to understand the material properties of the incorporated ashes. The mechanical properties of the concrete mixes were evaluated, and beams were made using the optimum mixes from the four ash proportions to investigate load capacity, deflection, ductility, and stiffness. A mathematical analysis was performed to calculate beam deflection and compare it with the experimentally obtained values. The failure mode observed during testing was analyzed to understand the behaviour of the HSRCB under load. The results reveal that the NRB4 mix, containing a specific combination of ash type, replacement level, and the presence of basalt fibre, exhibits optimal performance. NRB4 demonstrates superior load capacity, improved deflection control, enhanced ductility, and greater stiffness than other investigated mixes. This research highlights the potential of utilizing waste materials like MSWIA, nMSWIA, RHA, and nRHA in HSRCB production, promoting sustainable construction practices. Including basalt fibre further refines the mechanical properties, making NRB4 a promising mix for HSRCB applications.

Keywords: High-strength reinforced concrete beam; Mechanical properties; Ductility; Stiffness; Deflection; Scanning electron microscope.

1. INTRODUCTION

The demand for more robust, durable, and sustainable structures has led to a significant evolution in material technology in the construction industry in recent years. High-strength concrete (HSC) has emerged as a critical player in this arena, offering enhanced mechanical properties that make it ideal for various structural applications. However, the inherent brittleness of HSC remains a concern, particularly in scenarios where dynamic loading or sudden impact is a possibility. Researchers and engineers have turned to fibre reinforcement as a viable solution to mitigate this limitation. Many researchers explored the potential of using nano ashes and fibre to produce HSC for rigid pavements. Incorporating nanoash can significantly enhance the compressive and flexural strength of concrete compared to conventional mixes [1, 2]. High-strength concrete using nano ash and fibre presents a promising approach for achieving superior performance and promoting sustainable construction practices [3]. The development of high-strength concrete with enhanced compressive performance through short, straight steel fibres [4]. Utilizing MSWIA in construction materials can become a viable and sustainable approach, reducing environmental impact, potentially lowering costs, and contributing to a more circular economy in the construction sector [5]. Results indicate that concrete mixtures incorporating Municipal solid waste incinerator bottom ash (MSWIBA) exhibit comparable or enhanced performance characteristics under certain conditions [6]. MSWIBA can effectively improve strength and durability, making them a viable alternative to traditional building materials. It helps reduce the environmental impact of waste disposal and conserve natural resources [7, 8]. Adequately sized and graded MSWIBA particles can improve the packing density of concrete

Corresponding Author: Ananthakumar Ayyadurai Received on 24/05/2025 Accepted on 10/09/2025

DOI: https://doi.org/10.1590/1517-7076-RMAT-2025-0465

mixtures, reducing voids and enhancing the overall strength and workability of the concrete [9]. Adding water-treated MSWIBA to blended cement pastes could influence the microstructure formation. This might involve examining changes in pore structure, hydration products, and interfacial transition zones between cementitious materials and aggregates [10, 11]. The optimal proportions of MSWIBA, ground granular blast furnace slag (GGBFS), and sodium silicate to achieve the desired strength performance in concrete mixes [12]. A well-optimized internal transition zone (ITZ) can enhance the bond between the aggregate and the cement matrix, improving strength properties [13]. The pozzolanic activity of MSWI bottom ash can contribute to additional cementitious hydration products, potentially enhancing concrete strength and durability [14, 15].

The rice husk ash likely acts as a supplementary cementitious material in the geopolymer binder, contributing to the formation of additional hydration products and improving concrete strength [16]. Sustainable concrete incorporating RHA offers environmental benefits by reducing the demand for cement, which in turn lowers emissions of CO_2 related to the manufacturing of cement. RHA can enhance concrete properties such as compressive strength, durability, and workability when used in appropriate proportions [17, 18]. Rice husk ash acts as a supplementary cementitious material in the geopolymer binder, contributing to the formation of additional hydration products and improving concrete strength. It contributes to forming additional hydration products, enhancing concrete strength and durability [19]. It provides insights into using RHA in sustainable concrete production and offers efficient methods for predicting concrete strength [20]. Its incorporation contributes to sustainability by reducing cement consumption lowering carbon emissions and energy consumption associated with cement production [21].

Basalt macro fibres are typically added to concrete mixes to improve tensile and flexural strength, control cracking, and enhance ductility [22]. These fibres, derived from natural basalt rock, offer high tensile strength and shear modulus, contributing to improved mechanical properties of the concrete. The effectiveness of basalt minibars in enhancing the shear strength and performance of BFRP-reinforced high-strength concrete beams [23]. Chopped basalt fibres are short-length fibres derived from natural basalt rock and added to concrete mixes to improve various mechanical properties [24]. Basalt Fibre-Reinforced Concrete (BFRC) can also improve the blast resistance of protected buildings by mitigating the effects of explosions and minimizing damage to structural elements [25]. The potential benefits of using BFRC include enhanced crack resistance, improved durability, and reduced environmental impact through the utilization of recycled materials [26, 27]. Shear capacity, crack formation, crack propagation, and failure modes are examined under different loading scenarios to assess the effectiveness of the basalt fibre-reinforced polymer (BFRP) reinforcement and basalt fibres in enhancing shear resistance [28-30]. Natural fibres can enhance concrete tensile strength, crack, and impact resistance, improving overall mechanical properties [31]. Integrating normal-weight and lightweight concrete in beam construction can significantly improve flexural strength without compromising structural integrity, offering a balanced solution for strength and weight optimization [32]. The use of Municipal Solid Waste Incineration Bottom Ash (MSWI-BA) in reinforced concrete beams found that, with proper mix design, MSWI-BA can enhance structural performance while promoting sustainable waste utilization [33]. Natural fibres (NFs) in structural concrete, highlight their positive effects on crack control, ductility, and environmental performance, while also emphasizing the need for optimized fiber dosage and dispersion techniques [34].

The expanding importance of fracture mechanics in structural design is highlighted by this gap analysis on fracture energy-based concrete design, which also identifies areas that require more research, especially when mixed-mode stress is present [35]. Fibrous alkali-activated concrete's (AAC) fracture behavior under Mode I, I/III, and III loading conditions shows how well sustainable activators and fibers work to increase crack resistance [36]. An inventive method for one-part geopolymer concrete that reports improved fracture toughness and promotes its potential for sustainable building is the synthesis of alkali activators from industrial waste [37]. Reactive powder concrete (RPC) ferrocement hollow beams' flexural performance showed that mesh type has a major impact on ductility and load-carrying capability [38]. Recycled aggregates in alkali-activated slag concrete have been found to decrease flexural strength, however this impact can be counteracted by appropriate mix design [39]. Steel fibers greatly increase flexural capacity and crack resistance in steel fiber reinforced high-strength concrete (SFRHC) beams, according to both experimental and numerical investigations [40]. Composite action enhances stiffness and ultimate load capacity, as demonstrated by bonded steel-concrete composite beams [41]. The microstructural behaviour and strength of geopolymer concrete based on fly ash, both binary and ternary. According to their research, using several binders improves microstructural refinement and strength growth [42]. The combined use of fly ash and recycled aggregates improves concrete's mechanical performance and sustainability [43]. Fly ash improves the hydration process and increases the long-term compressive strength of blended cements [44]. Activated carbon powder alters the air-void structure in fly ash concrete, affecting its workability and durability [45]. Concrete's strength retention and thermal resistance at high temperatures are enhanced by the addition of fly ash and metakaolin [46]. Using sustainable materials, including adding water

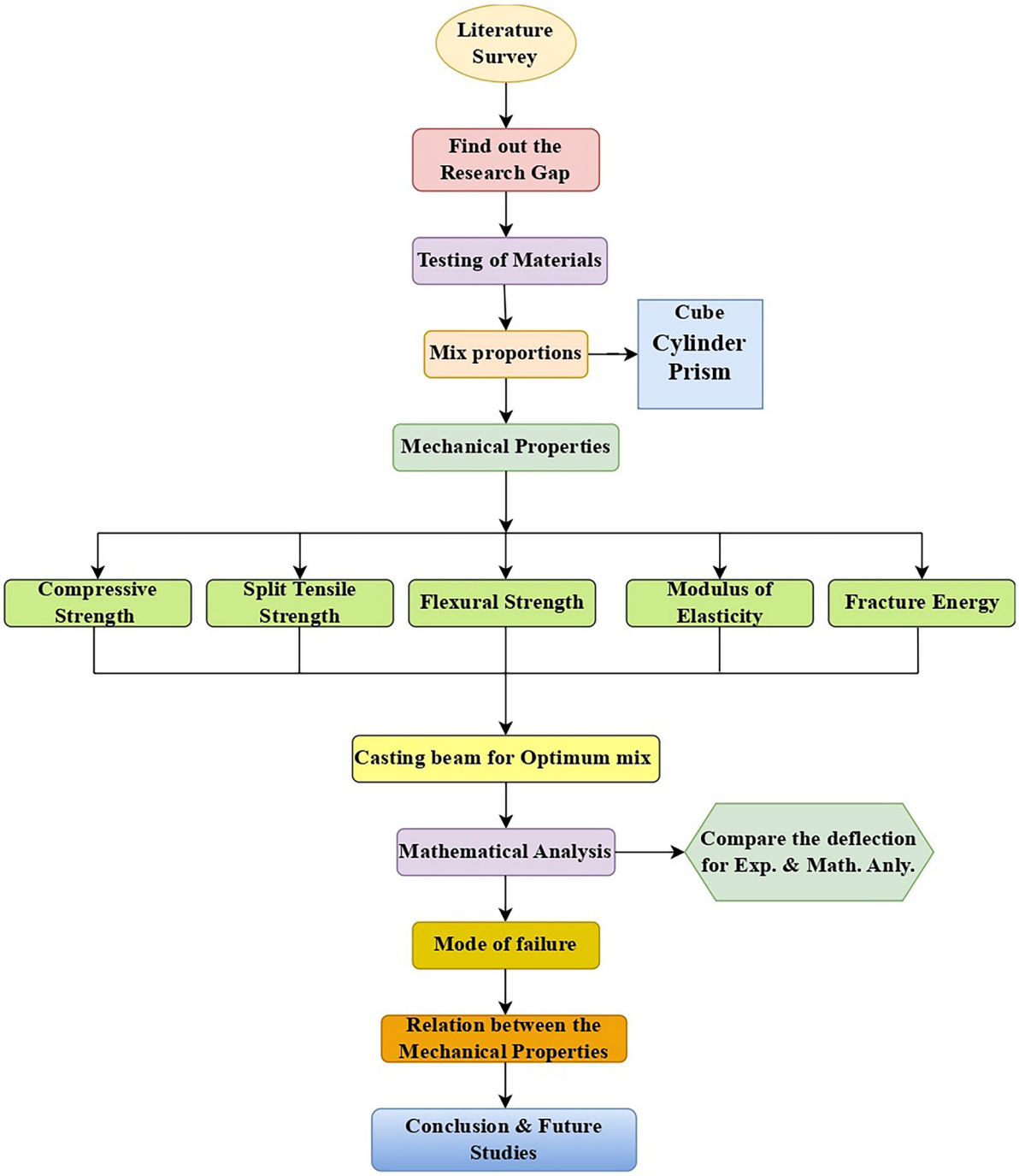


Figure 1: Research methodology.

hyacinth systems to concrete, may enhance its strength and durability [47]. The performance properties of self-compacting concrete have been demonstrated to be enhanced by the addition of silica fume and waste from marble cutting slurry [48]. The overall research methodology adopted in this study is illustrated in Figure 1.

This study investigates the novel integration of nanoscale waste-derived additives (nMSWIA and nRHA) with basalt fibres in high-strength reinforced concrete beams (HSRCB) to enhance both material and structural performance. While traditional research has largely focused on either pozzolanic replacements or fibre reinforcement individually, this work uniquely combines nano-engineered waste ashes with fibre reinforcement to achieve simultaneous improvements in microstructural refinement, durability, and load-bearing capacity. The hypothesis is that nano-additives, owing to their ultrafine particle size and high reactivity, will enhance hydration, densify the cement matrix, and synergize with basalt fibres to improve stiffness, ductility, and ultimate load capacity of HSRCBs, thereby offering a sustainable and high-performance alternative to ordinary concrete.

It explores a wide range of mix pro-portions; incorporating different replacement levels (5%, 10%, 15%, 20%, 25%, and 30%) for each type of ash. Additionally, the effects of including 0.5% basalt fibre are assessed. An analysis using an SEM is carried out to comprehend the characteristics of the integrated ashes. This detailed material characterization aids in correlating the ash's composition with the resulting mechanical performance of the concrete mixes. The mechanical properties are extensively evaluated, with the researchers measuring factors such as load capacity, deflection, ductility, and stiffness. Notably, the study progresses beyond solely evaluating the material properties of the concrete mixes. Beams are fabricated using the optimal mixes from each ash type, allowing a real-world assessment of their structural behaviour under load.

2. MATERIALS AND METHODS

2.1. Characterization of materials

Cement, a crucial constituent of concrete, determines its properties. This study employed Ordinary Portland Cement (OPC) of 53 Grade. The specific gravity of the cement, a key parameter influencing its behaviour in concrete, was determined to be 3.15. Testing procedures followed the guidelines outlined in IS: 4031 – 1988. The fineness and normal consistency of OPC are 6% and 31%. The setting time is mainly considered for concrete in construction. Based on the test, OPC's initial and final settings are 35 minutes and 320 minutes. The compressive strength of the OPC 53 grade is 54.60 MPa. The fine aggregate demonstrated a fineness modulus of 2.86 and a specific gravity of 2.65. The bulk density of fine aggregate is 1680 kg/m^3. Coarse aggregate, collected from crushed stone aggregates, was angular and partially uniform, measuring 20 mm. The test procedure for coarse aggregate adhered to IS: 2386-1963 standards. An important parameter, the coarse aggregate's specific gravity, was 2.74. The specifications outlined in IS: 383-1970, and the water absorption of the coarse aggregate was 0.65%. Aggregate impact and crushing strength parameters were found based on the laboratory test to be 12.2% and 27.12%. Superplasticizers, essential for improving the workability of concrete, were utilized in this study. The chosen plasticizer was naphthalene-based and complied with IS 9103-1999, BS: 5075 Part 3, and American Society for Testing and Materials (ASTM) C - 494 standards.

The MSWIA is collected from Erode Municipality Corporation. MSWIA is produced through grinding using a ball mill. The physical parameters of pH value and bulk density value of MSWIA and nMSWIA were determined to be 10.70 and 1.17 gm/cc. RHA, a key supplementary material, was produced by subjecting rice husks to a 48-hour open combustion process. The resulting ash, exhibiting a grey appearance, underwent further processing in a ball mill using the Box-Behnken method. This process generated micro-sized particles of RHA. Additionally, nRHA was produced by grinding the rice husk in a ball mill, resulting in much finer particles than regular RHA. The chemical compositions of the RHA, nRHA, nMSWIA, and MSWIA are displayed in Table 1. When compared to conventional cement, the usage of nRHA and nMSWIA in concrete gives considerable cost savings. RHA and MSWIA, which are made from municipal and agricultural waste, have processing prices ranging from INR 2,500 to INR 3,800 per ton, including treatment and grinding, whereas OPC costs between INR 6,000 and 7,500 per ton. The energy required for nano-sizing notwithstanding, these materials are 40–60% more cost-effective than OPC. Furthermore, they improve the strength and durability of concrete performance. Their use not only lowers the cost of materials but also promotes sustainable building by reducing carbon emissions from cement manufacture and landfill waste.

Natural fibres give cementitious composites better mechanical and durability qualities while providing environmentally friendly substitutes for conventional fibres. These fibres are superior to their conventional counterparts in many ways. They are cost-effective, biodegradable, non-toxic, easily accessible, non-abrasive, lightweight, and exhibit outstanding resistance to corrosion and fatigue. They also have a strong sense of specific strength [30]. Natural fibers including basalt, coconut, banana, bagasse, hemp, kenaf, bamboo, jute, sisal, abaca, and cotton are commonly utilized in cement-based composites because of their mechanical and environmental advantages. Basalt fiber was chosen for this investigation due to its exceptional endurance and mechanical qualities. Basalt fibers are derived from volcanic rock and processed into chopped strands. They have exceptional

Table 1: Chemical composition of MSWIA, nMSWIA, RHA and nRHA.

MATERIAL	LOI %	SiO_2 %	CaO %	MgO %	Fe_2O_3 %	Al_2O_3 %	Na_2O %	K_2O%
MSWIA	5.62	54.32	19.14	0.72	1.20	4.32	–	–
nMSWIA	1.42	68.52	20.14	0.92	1.38	7.60	–	–
RHA	7.27	82.89	0.76	0.97	0.53	1.68	0.20	–
NRHA	0.69	90.48	1.22	1.56	0.72	3.40	0.31	–

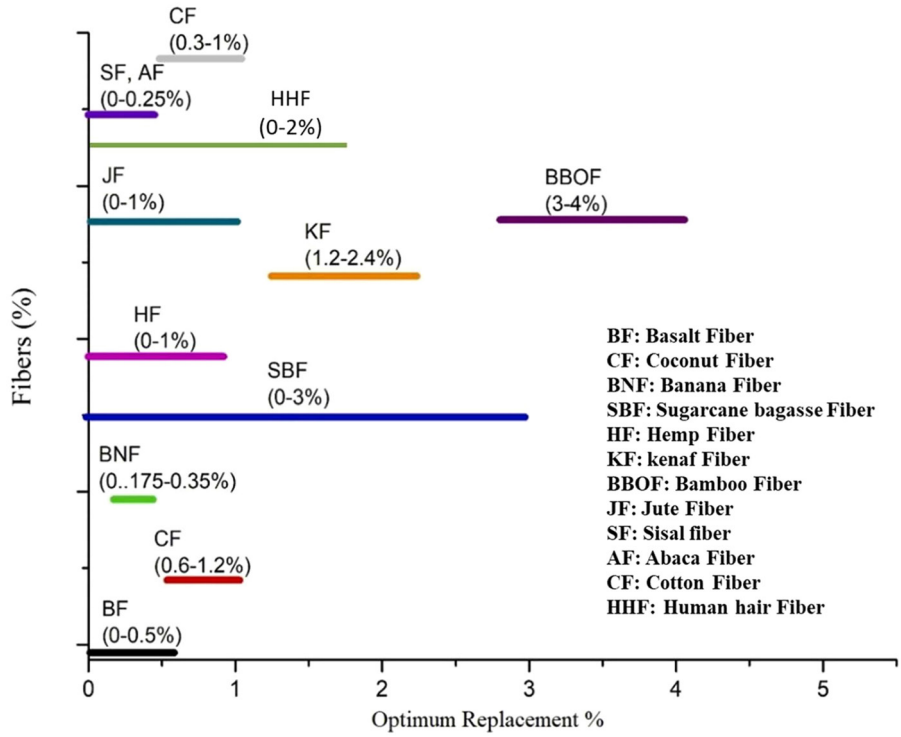


Figure 2: Optimal substitution ratio of different types of natural fibres in cement concrete [30].

heat stability and tensile strength. The fibers employed in this study had an aspect ratio of 1230, a diameter of 0.013 mm, and a length of 16 mm. Basalt fibers improve crack resistance, energy absorption, and flexural strength in high-strength concrete, making them perfect for structural applications needing increased durability and toughness. They have a density of 2.65 g/cm^3 and a tensile strength of 4150 MPa. Furthermore, basalt fibers are environmentally safe, chemically stable, and resistant to corrosion, all of which enhance their appropriateness for environmentally friendly building. Figure 2 illustrates the optimal substitution ratio of various natural fibres incorporated in cement concrete.

A thorough life cycle assessment (LCA) has been included to measure the environmental impact reduction attained by using basalt fibers, MSWIA, and nRHA in high-strength concrete. This is done to bolster the study's practical significance and environmental depth. In comparison to the control mix, the modified concrete mix shows a significant reduction in energy consumption (~33%) and carbon emissions (~31%), as well as a significant diversion of waste from landfills. Additionally, the updated discussion now covers real-world issues including the cost of processing and geographic availability of basalt fibers and nano-additives, especially in developing nations. These improvements highlight the sustainability and viability of using the suggested mix in actual construction applications and provide a more comprehensive assessment of cost-performance trade-offs.

2.2. SEM analysis

SEM is a method of microscopy in which a concentrated electron beam is used to scan a sample's surface. By interacting with the atoms in the sample, the electrons produce a variety of signals that can be utilized to identify the surface. SEM can provide information about the morphology (shape and size) of the sample, as well as its chemical composition. The four images show MSWIA, nMSWIA, RHA and nRHA at 250°C and 800°C. It is important to note that the scale of the image is different between the 1000x and 10,000x magnifications.

The MSWIA and RHA particles appear more oversized and irregular, with a rough and uneven texture. They are composed of various fused materials during incineration. In contrast, the nMSWIA and nRHA particles are smaller and more spherical, with a smoother surface. Suggests that they are formed through a different process, such as mechanical grinding or milling, which can break down larger particles into smaller ones.

The morphology of the MSWIA and nMSWIA appears to be more irregular than the RHA and nRHA (Figure 3). The MSWIA is derived from various materials, while RHA is more uniform. The nMSWIA appears to be smaller than the MSWIA. The nMSWIA was incinerated at a higher temperature (800^{0}C), which caused

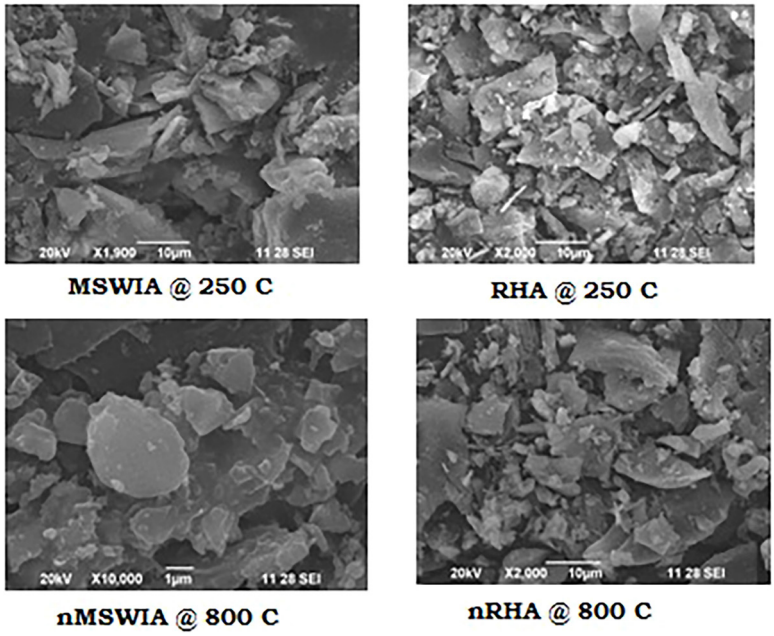


Figure 3: Morphology of MSWIA, RHA, nMSWIA and nRHA.

the particles to break down into smaller sizes. It is difficult to say definitively whether the nRHA is smaller than the RHA from the SEM images. Similarly, the scale of the image is different for the RHA and nRHA.

At higher temperatures, some of the volatile components in the ash may vaporize and escape as gases, leading to a decrease in the overall concentration of these elements. High incineration temperatures can also cause some of the inorganic components in the ash to decompose or react with each other. For instance, calcium carbonate ($CaCO_3$) decomposes at around 800^0C. If MSWIA or RHA contains a significant amount of $CaCO_3$, it is likely to decompose at higher incineration temperatures, forming CaO and CO_2. The formation of new compounds can alter the overall chemical properties of the ash, such as its reactivity, leaching behaviour, and pozzolanic activity.

2.3. Mix proportions

The materials used in this study included potable water, clean river sand for the fine aggregate, coarse aggregate with a maximum size of 20 mm, and ordinary Portland cement grade 53. Furthermore, the utilization of different admixtures such as municipal solid waste incineration ash, nano municipal solid waste incineration ash, rice husk ash, and nano rice husk ash to partially replace cement at varying levels of 5%, 10%, 15%, 20%, 25%, and 30% has been explored. Additionally, the effects of incorporating basalt fibre at a rate of 0.5% on these replacement levels have also been investigated. The following (Table 2) illustration explains the different mixes used for the study. In total, 24 mixes arrive by adding basalt fibre (MB1 to MB6, NMB1 to NMB6, RB1 to RB6 and NRB1 to NRB6). Figure 4 delves into the manufacturing and curing processes of all specimens.

2.4. Test methods

This experiment investigated the mechanical properties of high-strength concrete containing different amounts of basalt fibres. For each mix proportion, three cubes, three cylinders, and three prisms were cast and tested for mechanical properties after 28 days of curing. The cubes (100mm × 100mm × 100mm), cylinders (100mm × 20mm), and chromatic samples (500mm × 100 × 100mm) were tested to determine their compressive strength (CS), split tensile strength (STS), flexural strength (FS). The mechanical test results of all specimens were used to identify the optimum mix proportion. With this selected mix, beam specimens of 1000 mm × 100 mm × 150 mm were cast and tested under a three-point bending setup to examine their deflection behaviour under loading. The experiment also examined how the type and amount of fibres affected the concrete's compressive and tensile behaviour and fracture energy.

CS is a crucial metric for concrete as it reflects its capacity to withstand compressive loads. In this investigation, cube-shaped specimens measuring 100mm on each side were subjected to a CS test following a 28-day curing period. This curing timeframe allows the concrete to achieve a significant portion of its potential strength. The test procedure adhered to the PN-EN 12390-3:2002 standard, ensuring consistency and reliable results. A

Table 2: Mix Proportions for MSWIA, nMSWIA, RHA, and nRHA mixes per m^3 of concrete.

MIX ID	CEMENT (kg)	FA (kg)	CA (kg)	MSWIA (kg)	nMSWIA (KG)	RHA (kg)	nRHA (kg)	Basalt (%)	W/B RATIO (Lit.)	SUPER PLASTICIZER (%)
CC	350	717	1356	0	–	–	–	0	140	0
MB1	332.5	717	1356	17.5	–	–	–	0.50	140	1
MB2	315	717	1356	35	–	–	–	0.50	140	1
MB3	297.5	717	1356	52.5	–	–	–	0.50	140	1
MB4	280	717	1356	70	–	–	–	0.50	140	1
MB5	262.5	717	1356	87.5	–	–	–	0.50	140	1
MB6	245	717	1356	105	–	–	–	0.50	140	1
NMB1	332.5	717	1356	–	17.5	–	–	0.50	140	1
NMB2	315	717	1356	–	35	–	–	0.50	140	1
NMB3	297.5	717	1356	–	52.5	–	–	0.50	140	1
NMB4	280	717	1356	–	70	–	–	0.50	140	1
NMB5	262.5	717	1356	–	87.5	–	–	0.50	140	1
NMB6	245	717	1356	–	105	–	–	0.50	140	1
RB1	332.5	717	1356	–	–	17.5	–	0.50	140	1
RB2	315	717	1356	–	–	35	–	0.50	140	1
RB3	297.5	717	1356	–	–	52.5	–	0.50	140	1
RB4	280	717	1356	–	–	70	–	0.50	140	1
RB5	262.5	717	1356	–	–	87.5	–	0.50	140	1
RB6	245	717	1356	–	–	105	–	0.50	140	1
NRB1	332.5	717	1356	–	–	–	17.5	0.50	140	1
NRB2	315	717	1356	–	–	–	35	0.50	140	1
NRB3	297.5	717	1356	–	–	–	52.5	0.50	140	1
NRB4	280	717	1356	–	–	–	70	0.50	140	1
NRB5	262.5	717	1356	–	–	–	87.5	0.50	140	1
NRB6	245	717	1356	–	–	–	105	0.50	140	1



Figure 4: Manufacturing of concrete specimens and curing process.

compressive testing machine (CTM) with a capacity of 2000kN accommodates the anticipated forces during the test and ensures accurate measurement of the concrete's compressive capability. The indirect tensile strength, also known as STS, was evaluated by PN-EN 12390-6:2001. Cylindrical specimens with a diameter of 100 mm and a length of 200 mm were cast and cured for 28 days before testing on a CTM. FS, known as three-point

bending strength, was determined according to EN 12390-5:2009. Specimens measuring 100 mm wide, 100 mm deep, and 500 mm long were tested after 28 days of curing. A central load was applied to the specimens with a support span of 300 mm. The static modulus of elasticity was measured on cylindrical specimens after completing the curing process. The testing adhered to ASTM C469-02:2004 standards and employed an extensometer to gauge deformations.

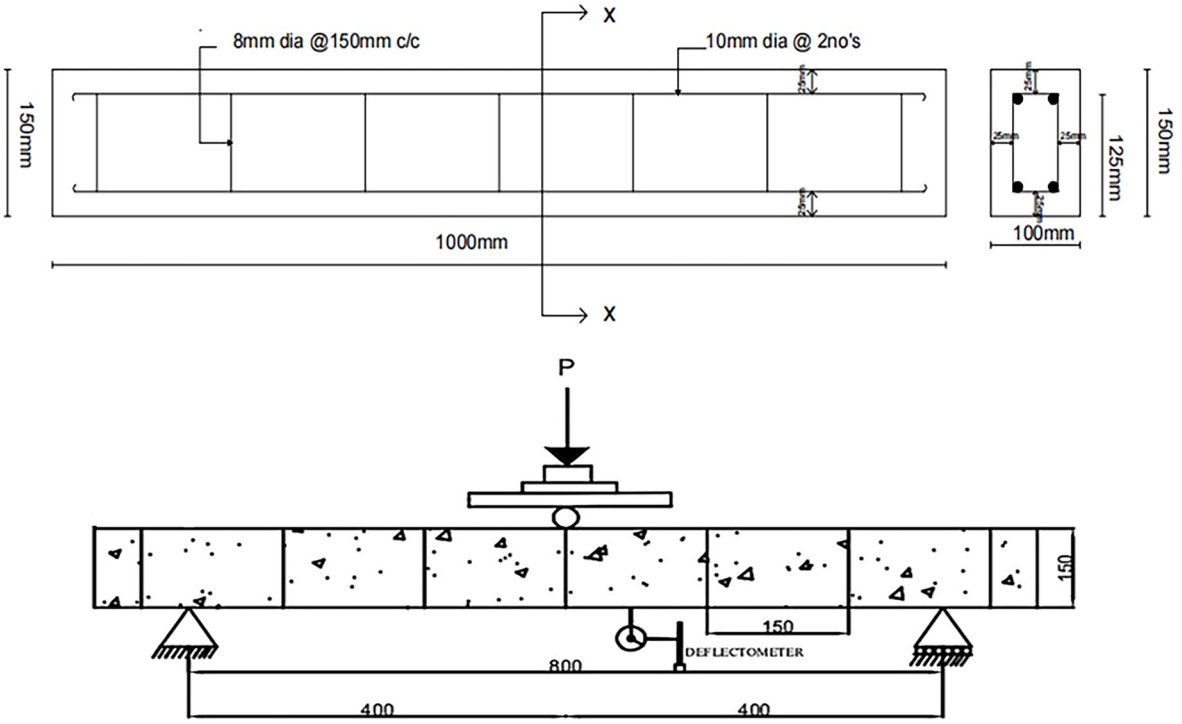


Figure 5: Reinforcement details and single-point load setup model.

Table 3: Equations for determining tensile stress and fracture energy.

STRENGTH PARAMETERS	EQUATION
HSC	
Stress intensity factor	$K_{Ic} = \frac{F_{max}}{b\sqrt{h}} f(\alpha)(MN/m^{1.5})$
Geometry function	$f(\alpha) = 6\sqrt{\alpha}\left(\frac{1.99-\alpha(1-\alpha)(2.15-3.93\alpha+2.7\alpha^2)}{(1+2\alpha)(1-\alpha)^{(3/2)}}\right)$
Fracture energy	$G_f = \frac{K_{IC}{}^2(1-v)}{E_c m}(N/mm)$
Fibre-reinforced HSRC	
Tensile stress	$\alpha = \frac{3Fl}{2b(h-\alpha_0)^2}(Mpa)$
Fracture energy	$G_f = \int_{\delta=\delta_i im}^{\delta=\delta_i im} \alpha d\delta (N/mm)$

The sample width (b = 100 mm), sample height (h = 150 mm), relative crack length ($\alpha = a_0/h$), notch depth (a_0 = 60 mm), Poisson's ratio (v), average static modulus of elasticity (E_{cm}), sample span (l = 1000 mm), distance between the notch tip and sample top edge ($h - a_0$), and load recorded during the three-point bending test (F_{max}).

After curing for 28 days, 1000 mm × 100 mm × 150 mm notched specimens were tested in three-point bend-ing following the RILEM TC 89-FMT guidelines. The reinforcement details are a 10mm diameter rod provided on the tension and compression zone. 8mm diameter and 150mm spacing were provided for the stir-rups the entire length of the beam (Figure 5). A constant displacement rate of 0.05 mm/min was applied using a deflectometer positioned at the base of the specimen. The determination of crucial fracture properties, namely the stress intensity factor (KIc) and fracture energy (GF), relied on established equations referenced in [42]. KIc characterizes the stress concentration near a crack tip, while GF quantifies the energy required for crack prop-agation. These parameters are critical for modelling the post-cracking stress-strain behaviour of high-strength concrete with basalt fibre. The testing methodology aligns with RILEM recommendation TC162-TDF [43], which acknowledges the influence of crack mouth opening displacement (CMOD) and fibre distribution on deflection variability, as substantiated by research documented in [44-46]. Equations for calculating FS and fracture energy in Fibre-reinforced HSRC are also provided in Table 3.

3. EXPERIMENTAL INVESTIGATION

Table 4 presents the properties of hardened concrete for all mix proportions and the percentage change in strength values compared to the maximum value recorded for each strength type.

Table 4: Hardened concrete properties of all mix.

MIX ID	CS (MPa)	% OF INCREASE/ DECREASE VARIATIONS OF CS	STS (MPa)	% OF INCREASE/ DECREASE VARIATIONS OF STS	FS (MPa)	% OF INCREASE/ DECREASE VARIATIONS OF FS
CC	42.24	–	3.52	–	4.86	–
MB1	49.23	0.00	3.95	0.00	4.92	0.00
MB2	48.65	1.18	3.84	2.78	4.85	1.42
MB3	47.12	4.29	3.64	7.85	4.73	3.86
MB4	45.15	8.29	3.52	10.89	4.62	6.10
MB5	42.35	13.98	3.43	13.16	4.52	8.13
MB6	41.26	16.19	3.25	17.72	4.40	10.57
NMB1	51.24	0.00	4.12	0.00	5.05	0.00
NMB2	49.24	3.90	3.86	6.31	4.92	2.57
NMB3	46.65	8.96	3.82	7.28	4.75	5.94
NMB4	46.05	10.13	3.64	11.65	4.62	8.51
NMB5	44.24	13.66	3.52	14.56	4.55	9.90
NMB6	42.76	16.55	3.35	18.69	4.76	5.74
RB1	42.12	18.45	4.16	13.69	5.10	4.85
RB2	43.12	16.52	4.35	9.75	5.24	2.24
RB3	46.43	10.11	4.42	8.30	5.30	1.12
RB4	51.65	0.00	4.82	0.00	5.36	0.00
RB5	45.34	12.22	4.10	14.94	5.18	3.36
RB6	41.63	19.40	3.84	20.33	4.76	11.19
NRB1	43.25	19.08	4.52	19.57	5.34	6.97
NRB2	44.75	16.28	4.75	15.48	5.46	4.88
NRB3	47.60	10.94	5.15	8.36	5.50	4.18
NRB4	53.45	0.00	5.62	0.00	5.74	0.00
NRB5	49.32	7.73	5.34	4.98	5.60	2.44
NRB6	44.50	16.74	4.82	14.23	5.52	3.83
Mean	45.97	–	4.13	–	5.03	–
SD	3.40	–	0.65	–	0.38	–
V	11.53	–	0.42	–	0.14	–
CI %	95.45	–	94.65	–	95.62	–

The CS of all the concrete mixes is between 41.26 MPa and 53.45 MPa. The mix with the highest CS is RB4 (51.65 MPa). The control mix (CC) has a CS of 42.24 MPa, close to the average CS of all the mixes (46.9 MPa). The percentage change in CS for the other mixes relative to the highest value (51.65 MPa) ranges from –19.40% to 0%. The STS of all the concrete mixes is between 3.25 MPa and 5.62 MPa. Mix RB4 also has the highest STS (4.82 MPa). The CC achieved a STS of 3.52 MPa, slightly lower than all the mixes' average split tensile strength (4.2 MPa). The percentage change in STS for the other mixes relative to the highest value (4.82 MPa) ranges from –32.36% to 0%. The FS of all the concrete mixes is between 4.40 MPa and 5.74 MPa. Mix RB4 also has the highest FS (5.36 MPa). The CC has an FS of 4.86 MPa, close to the average FS of all the mixes (5.0 MPa). The percentage change in FS for the other mixes relative to the highest value (5.36 MPa) ranges from –17.91% to 0%.

4. RESULT AND DISCUSSION

4.1. Fresh concrete properties

Slump is a standard test used in civil engineering to measure the workability of concrete mix. It is determined by moulding the concrete into a cone-shaped mould and then measuring how many slumps the concrete has after the mould is lifted. A higher slump value indicates the concrete is wet and fluid, while a lower slump value indicates the concrete is drier and stiffer. There is often a trade-off between slump and other properties of concrete.

Figure 6 reveals that the slump value of the different concrete mixes lies within a narrow band, ranging from 95 mm to 104 mm, thereby indicating that all mixes demonstrated satisfactory workability with only minor variations. The CC recorded a slump value of 101 mm, which serves as the reference for comparison across all modified mixes. In the case of the MB mixes, slump values varied between 98 mm and 101 mm, showing only a 3 mm spread within the group. Importantly, the highest slump value in the MB category was only 3 mm lower than the CC mix, suggesting that the inclusion of basalt fibres with municipal solid waste ash produced only a marginal reduction in workability.

A similar trend is observed in the NMB mixes, which also recorded slump values between 98 mm and 101 mm, mirroring the variation seen in MB mixes. The RB mixes followed the same pattern, falling within the 98 mm to 101 mm range, indicating that the addition of rice husk ash along with fibres did not cause significant deviations in fresh concrete behaviour compared to the CC mix. On the other hand, NRB mixes exhibited slightly lower slump values, ranging from 95 mm to 99 mm. This group was the only one where the maximum slump value fell below that of the CC mix, showing a slightly greater impact of nano-additives and fibre interaction on workability. Despite this reduction, the lowest recorded slump value of 95 mm (NRB6) corresponds to only a 6% decrease relative to the CC mix, while the highest slump values of 101 mm (MB6 and NMB6) correspond to a 3% increase. Taken together, these results confirm that the variation in slump across all mixes is relatively small and remains within acceptable limits, ensuring ease of placement and compaction.

4.2. CS of HSC

The MB mixes exhibit CS's ranging from 41.26 MPa to 49.23 MPa, reflecting a decrease of 20.14% to 4.64% relative to the optimal value of 51.65 MPa (Figure 7). Notably, none of the MB mixes surpass the optimal value,

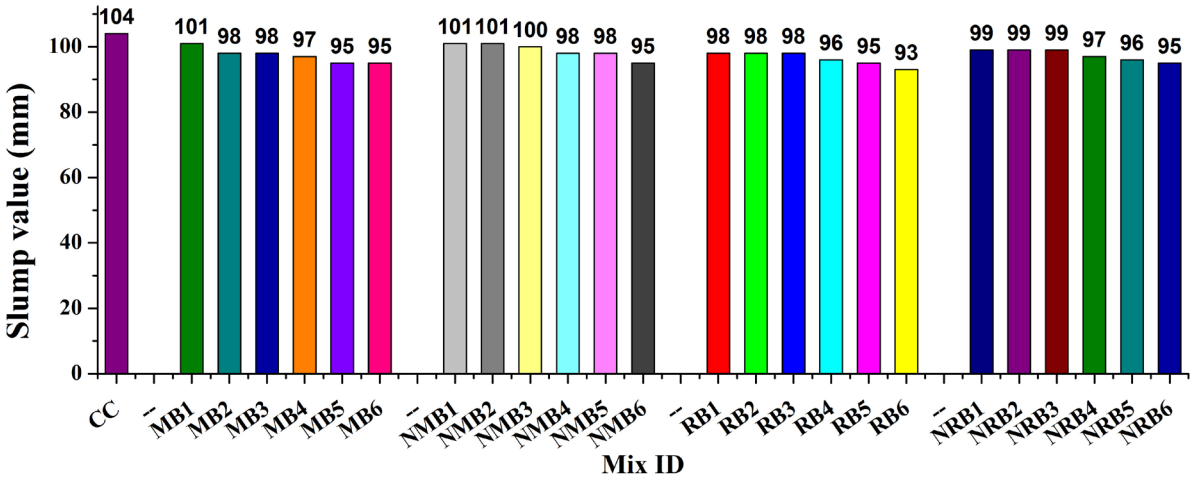


Figure 6: Slump value of all mix proportions.

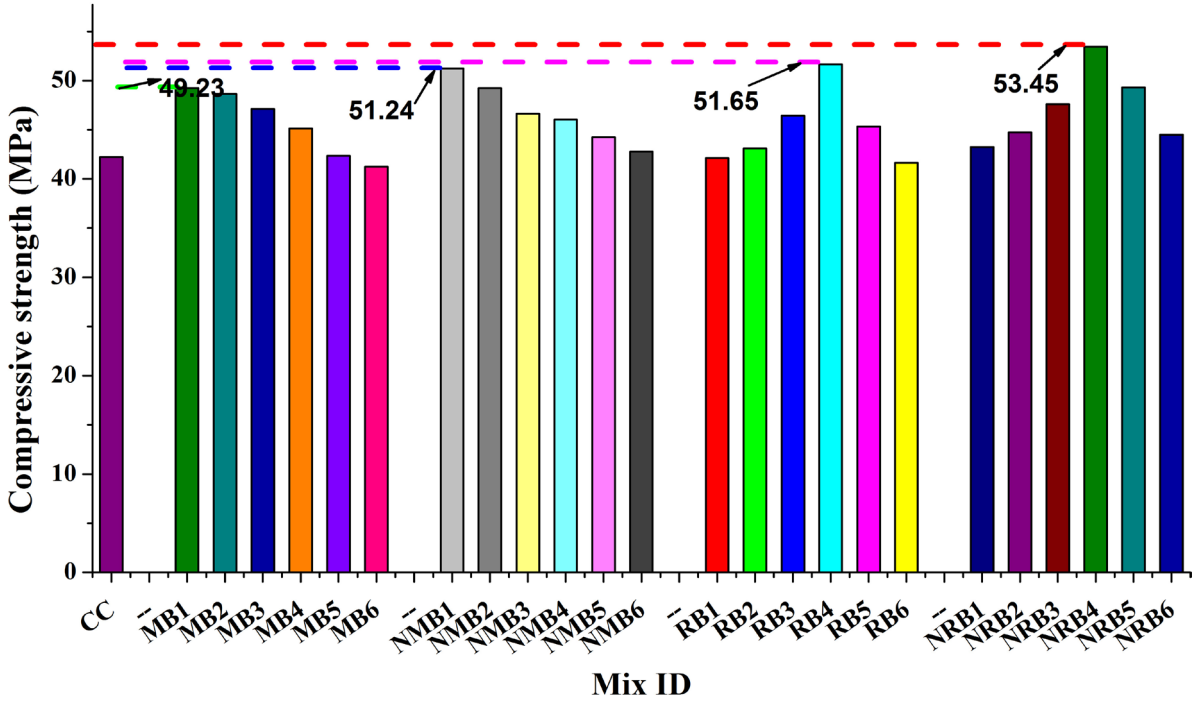


Figure 7: CS values of all cube specimens.

with MB1 coming closest at 49.23 MPa, which is 4.64% lower than the optimal. Previous studies have also observed that excessive incorporation of fibres without sufficient matrix densification can lead to reduced compaction and entrapped voids, thereby lowering compressive capacity [18]. In contrast, the NMB mixes exhibit compressive strength values ranging from 42.76 MPa to 51.24 MPa, indicating a reduction of up to 17.25% compared to the optimal, with one mix matching the optimal compressive strength. NMB1 is the only mix in this group to achieve the optimal CS of 51.24 MPa. The remaining NMB mixes fall below the optimal value, with decreases ranging from 4.64% to 17.25%.

The RB mixes exhibit the widest variation in CS, ranging between 41.63 MPa and 53.45 MPa. This spread represents reductions of 19.40% to 3.49% when compared with the optimal benchmark value. Among the RB group, RB4 demonstrated the highest compressive strength, recording 51.65 MPa, which was adopted as the reference optimum. Conversely, RB6 displayed the weakest performance within the group, showing a 19.40% decline relative to the optimum value. Such variability highlights the sensitivity of RHA–basalt fibre composites to fibre dosage and dispersion uniformity. These findings are consistent with previous literature reporting that basalt fibres improve compressive response primarily through crack control and enhanced matrix densification, but their efficiency depends heavily on achieving proper fibre alignment and adequate bonding with the cementitious matrix [22, 23]. Therefore, while the inclusion of RHA and basalt fibres provides clear structural benefits, ensuring consistent performance across different mix proportions remains a key challenge.

The NRB mixes, in contrast, demonstrated superior performance compared to RB blends, with CS values ranging from 43.25 MPa to 53.45 MPa. This corresponds to reductions of 16.30% to 3.49% relative to the benchmark optimum. Within this series, NRB4 achieved the highest compressive strength of 53.45 MPa, which not only surpassed the RB4 benchmark by 3.49% but also established the maximum strength among all tested mixes. This improvement can be attributed to the synergistic influence of nanoscale additives, which refine the pore structure, densify the interfacial transition zone (ITZ), and stimulate secondary hydration reactions. The resulting microstructural improvements enhance fibre–matrix interaction, leading to more effective stress transfer under compression [31]. The remaining NRB mixes recorded strength values below the optimum, with decreases ranging from 13.66% to 7.85%. Overall, the results confirm that while RB4 performed best among conventional blends, NRB4 demonstrated the most significant advancement, surpassing the optimum benchmark and underscoring the critical role of nano-additives in unlocking the full potential of fibre-reinforced composites.

4.3. STS of HSC

The STS results for the MB group highlight the limitations of MSWIA as a partial cement replacement when combined with basalt fibres. The six MB mixes achieved STS values ranging from 3.25 MPa to 3.95 MPa, which correspond to reductions of 32.36% to 18.03% compared to the optimum value (OV) of 4.82 MPa. None of the MB mixes surpassed the optimum benchmark, with MB1 recording the highest STS of 3.95 MPa, falling short by 18.03%. These results suggest that although MSWIA contributes to sustainability, its use in non-nano form does not fully enhance crack resistance or tensile load-carrying efficiency. The nano-modified MSWIA (NMB) mixes performed slightly better, with STS values ranging between 3.35 MPa and 4.12 MPa. NMB1 was the strongest performer within this series, with an STS of 4.12 MPa, which is 14.50% lower than the OV. While nano-modification refined the matrix, improving fibre anchorage and stress distribution, none of the NMB mixes exceeded the optimum strength, indicating the necessity of carefully balancing ash replacement levels and fibre dosage to maximize tensile benefits.

In contrast, the RHA-based mixes exhibited more promising performance. The RB group showed STS values ranging from 3.84 MPa to 4.82 MPa, with RB4 achieving the optimum benchmark of 4.82 MPa (Figure 8). This confirms the positive role of rice husk ash in enhancing tensile properties through improved pozzolanic reactivity and matrix densification. The variability among RB mixes, however, was significant, with RB2 recording the largest deviation at 20.10% below the OV. These findings are consistent with previous research, where fibre reinforcement enhanced crack bridging, and nanoscale additives further refined the matrix and improved toughness [28, 42]. The most substantial improvements were observed in the NRB mixes, which exhibited STS values between 4.16 MPa and 5.62 MPa. Notably, NRB4 exceeded the benchmark by 16.78%, achieving 5.62 MPa, the highest among all tested mixes. This enhancement reflects the synergistic effect of nanoscale additives and fibres in creating a denser microstructure, strengthening the interfacial transition zone, and resisting crack propagation. The remaining NRB mixes also displayed improved performance, though still below the optimum, with reductions between 13.69% and 7.89%. By comparison, the control mix (CC) lagged significantly, recording 3.52 MPa, which is 26.99% below the OV. These results clearly demonstrate that NRB4 is the most effective blend, combining waste-derived nanoscale additives and basalt fibres to significantly enhance tensile strength beyond conventional performance.

4.4. FS of HSC

Figure 9 presents the flexural strength (FS) results, highlighting that mix RB4 achieved the optimum value (OV) of 5.36 MPa, which is taken as the benchmark for comparison. In the case of MB mixes, the FS values fall within the range of 4.40 MPa to 4.92 MPa, which represents a reduction of 18.12% to 8.19% relative to the

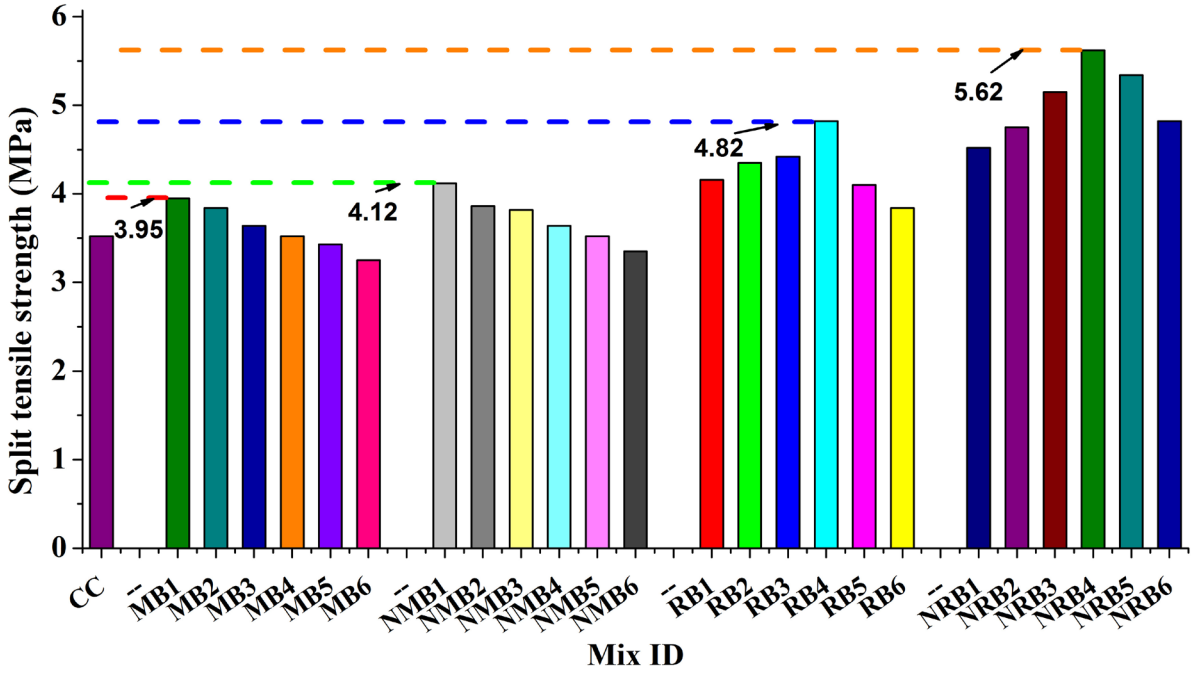


Figure 8: STS values of all cylinder specimens.

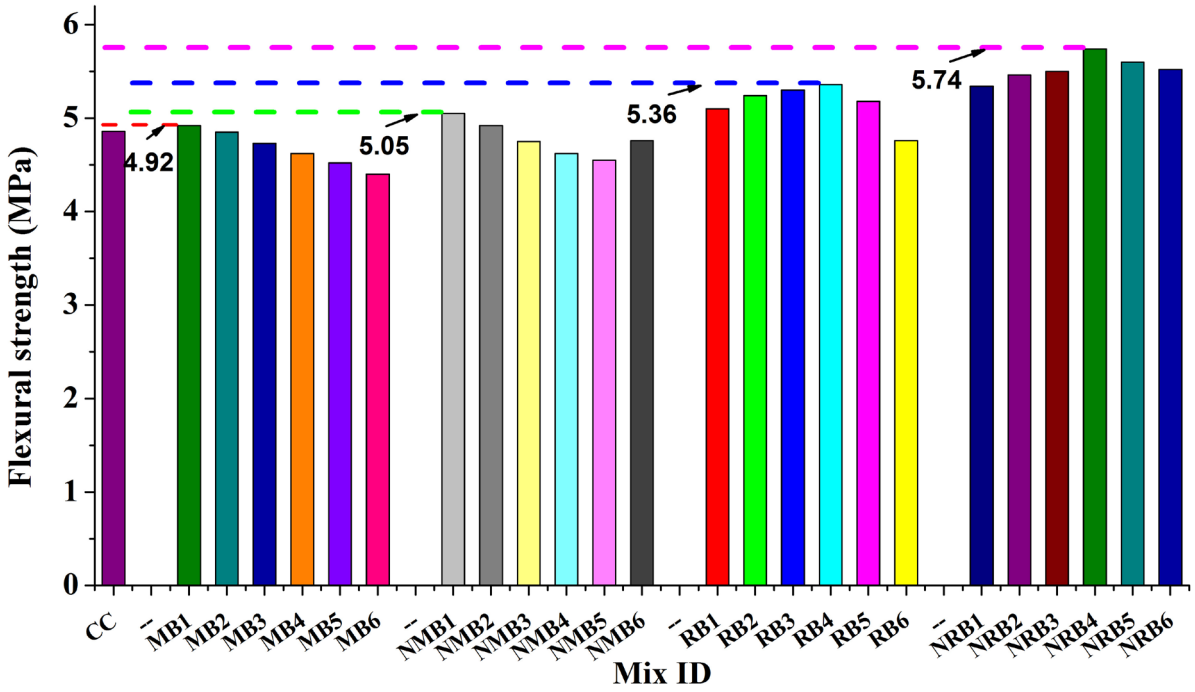


Figure 9: FS values of all prism specimens.

optimum. Among these, MB1 was the closest to the benchmark with an FS of 4.92 MPa, only 8.19% below the OV. These findings suggest that while the inclusion of municipal solid waste incineration ash (MSWIA) with basalt fibre (0.5%) contributes to strength development, it does not outperform other combinations, indicating that the synergy between fibre content and ash replacement requires fine optimization. Similarly, the nano-modified MSWIA (NMB) mixes showed FS values ranging from 4.52 MPa to 5.05 MPa. Although the nano-scale modification improved the matrix densification compared to MB mixes, the performance was still lower than the optimum benchmark, with NMB4 being the best performer at 5.05 MPa, just 5.79% lower than the OV. This highlights that nano-modification enhances flexural response, but alone it is not sufficient to exceed the maximum achievable strength.

The rice husk ash (RHA) series displayed a broader range of FS values, spanning from 4.55 MPa to 5.36 MPa. The optimum benchmark of 5.36 MPa was attained by RB4, making it the highest-performing mix in this group. This indicates that the correct balance of fibre reinforcement and RHA replacement can significantly enhance flexural performance. However, within the RB series, not all mixes achieved this synergy; RB1 deviated by 15.11% below the benchmark, showing that excessive replacement or poor fibre dispersion may limit strength development. The nano-RHA (NRB) series showed the most remarkable improvements, with FS values ranging between 4.76 MPa and 5.62 MPa. Notably, NRB4 exceeded the optimum benchmark by 4.85%, achieving 5.62 MPa, which is the highest among all tested mixes. This improvement can be attributed to the densification effect of nano-additives, which refine the pore structure, enhance fibre–matrix bonding, and improve stress redistribution during bending stresses [46]. The remaining NRB mixes, although not surpassing the benchmark, still performed strongly, with deviations ranging from 8.58% to 11.21% below the OV. Overall, the results confirm that the integration of nano-additives with basalt fibres, particularly in NRB4, maximizes flexural strength by combining enhanced crack resistance with superior load transfer efficiency.

4.5. Modulus of elasticity

This research investigates the modulus of elasticity (MoE) of high-strength concrete mixes incorporating basalt fibres. Cylindrical specimens with a standardized diameter of 150 mm and length of 300 mm were used for the experiment. To accurately measure the MoE, these cylinders were equipped with compressive and extensometer devices. The instrumented specimens were then placed in a CTM for data collection. The CTM recorded load and deflection data from all samples throughout the testing process. The experimental procedures strictly adhered to the established guidelines outlined in IS - 516: 1959 standards, ensuring the reliability and consistency of the results.

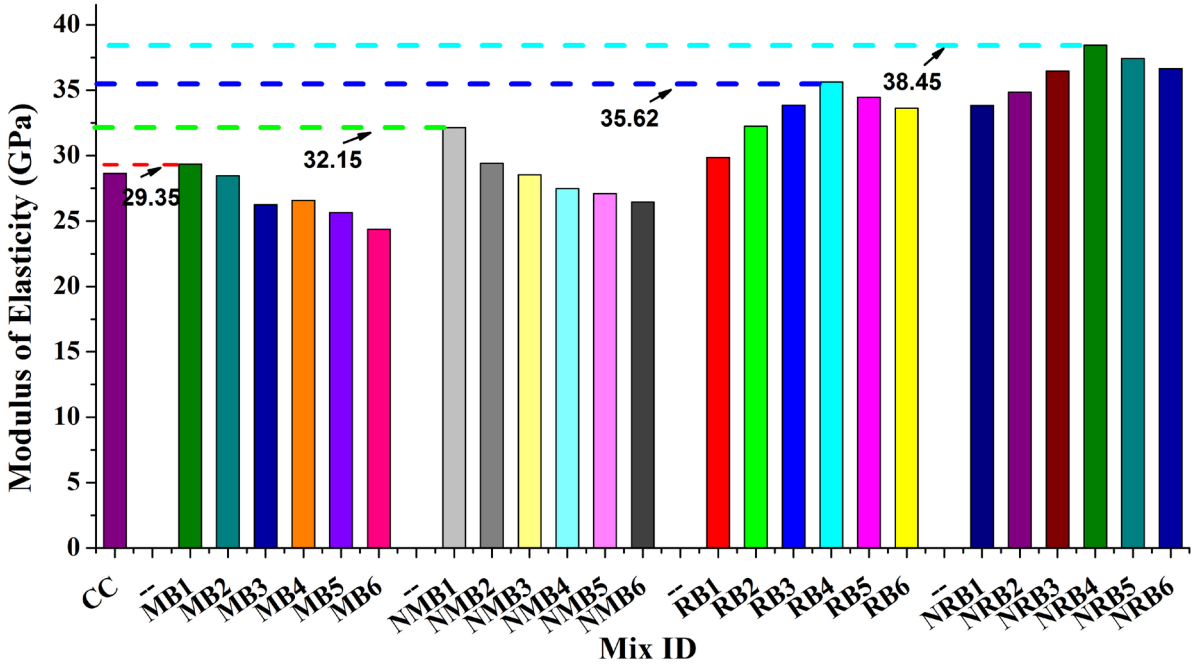


Figure 10: MoE of high-strength concrete for all mix.

Figure 10 presents the MoE values obtained for the different high-strength concrete mixes, clearly highlighting the variation in stiffness with respect to fibre incorporation and nano-additive usage. Among all the tested specimens, NRB4 achieved the highest MoE of 38.45 GPa, surpassing all other mixes and demonstrating superior stiffness. When compared to the baseline CC, which recorded the lowest values, NRB4 achieved an impressive 25.48% enhancement. Similarly, MB, NMB, and RB mixes also exhibited considerably higher MoE than the CC mix, indicating that basalt fibres, in combination with supplementary cementitious materials, substantially contribute to improved stiffness and better elastic performance.

The improvement in MoE for NRB4 and other mixes can be attributed to the refinement of the pore structure, densification of the matrix, and superior fibre–matrix interaction, all of which reduce microstructural weaknesses and enhance load transfer efficiency. Such characteristics are particularly valuable in structural applications that require high dimensional stability and minimal deformation under service loads. Previous research has consistently shown that nano-silica and RHA play a vital role in filling voids, reducing porosity, and strengthening the interfacial transition zone, which significantly boosts the stiffness of fibre-reinforced concrete [23, 25]. These findings suggest that NRB4, owing to its combined mechanical strength and high MoE, is especially well-suited for high-performance structural elements where both strength and rigidity are essential.

4.6. Fracture energy

This section of the research delves into the influence of fibre content on the equivalent flexural strength and fracture energy of HSRCB. The evaluation process solely focused on the fibres' impact, aiming to isolate their contribution to these crucial mechanical properties. Table 5 serves as a central component of this analysis. It presents the average values for three key parameters measured during the experiment: fracture load, deflection, and energy absorption. Each value represents the average performance observed across HSRCBs that incorporated fibre contents and exhibited varying micro-crack widths.

CC contains no basalt fibres, and observed baseline fracture energy of 12.152 N/mm. This value is used as a reference point to evaluate the performance improvements brought by including basalt fibres under different conditions. A notable increase in fracture energy is evident for the MB mixes, where fibres are added and subjected to monotonic loading. For instance, MB1 (0.25% fibre content) shows a 98.27% increase in fracture energy compared to the control. This trend continues with MB2 (0.5%) and MB3 (0.75%), which exhibit 106.82% and 123.59% increases, respectively. However, as the fibre content increases further in MB4, MB5, and MB6, there is a relative decrease in fracture energy compared to MB3, though these mixes still show significant improvements over the control, with increases of 81.85%, 78.17%, and 66.58%, respectively. The optimal

Table 5: Average values of HSRCB structural analysis parameters.

SPECIMEN ID	BASALT FIBRE CONTENT (%)	FL (kN)	FMAX (kN) EXPT.	AVG FRACTURE ENERGY (N/mm)
CC	0	1.22	6.55	12.152
MB1	0.5	3.54	6.65	26.406
MB2	0.5	3.20	6.53	24.102
MB3	0.5	2.82	5.86	23.840
MB4	0.5	2.58	5.45	23.456
MB5	0.5	2.75	5.10	21.650
MB6	0.5	2.33	4.85	20.652
NMB1	0.5	4.12	7.96	28.651
NMB2	0.5	3.80	7.65	28.152
NMB3	0.5	3.65	7.21	27.412
NMB4	0.5	2.98	6.75	26.410
NMB5	0.5	2.62	6.20	25.756
NMB6	0.5	2.54	5.86	25.412
RB1	0.5	3.53	6.25	26.745
RB2	0.5	3.85	7.63	28.230
RB3	0.5	4.66	8.92	30.154
RB4	0.5	5.25	10.26	32.450
RB5	0.5	4.30	9.25	31.256
RB6	0.5	4.16	7.98	30.145
NRB1	0.5	5.28	8.85	32.471
NRB2	0.5	6.83	9.89	34.120
NRB3	0.5	7.35	10.24	34.650
NRB4	0.5	8.58	12.65	35.480
NRB5	0.5	8.27	11.32	34.856
NRB6	0.5	7.62	10.25	33.564
Mean				27.93
Standard Deviation (SD)				5.37
Vairance				28.87

fibre content is around 0.75% for the highest fracture energy under monotonic loading. The NMB mixes, which involve various fibre contents under monotonic loading, exhibit even higher fracture energies. NMB1 (0.25%) achieves a 135.88% increase, and this upward trend continues, reaching a peak with NMB6 (0.75%) at 142.71%. These results indicate that normal-strength concrete combined with basalt fibres performs better in fracture energy than the standard high strength mix, particularly as the fibre content approaches 0.75%.

In the RB mixes, where the beams were subjected to repeated loading, the improvements in fracture energy were particularly significant. For instance, RB1 (0.25%) exhibited a 148.24% increase, while RB6 (0.75%) recorded a 164.65% increase. This trend can be attributed to the role of basalt fibres in bridging micro-cracks, restricting their widening, and distributing stresses more uniformly under cyclic loading conditions (Figure 11). Such fibre activity enhances the ability of the concrete to absorb energy before failure. SEM examinations provided further evidence by showing that the addition of nMSWIA and nRHA refined the pore structure and contributed to a denser cementitious matrix. The refined microstructure not only reduced weak points within the material but also improved the bond between fibres and the surrounding matrix. This stronger fibre–matrix interface limited fibre pull-out, increased anchorage, and ultimately allowed more energy to be dissipated during crack propagation.

The NRB mixes, on the other hand, demonstrated the highest levels of fracture energy among all the tested specimens. For example, NRB1 (0.25%) achieved a 167.23% increase, while NRB4 (0.75%) reached an impressive 191.39%. Even the intermediate mix NRB5 (0.5%) showed a substantial improvement of 175.14%.

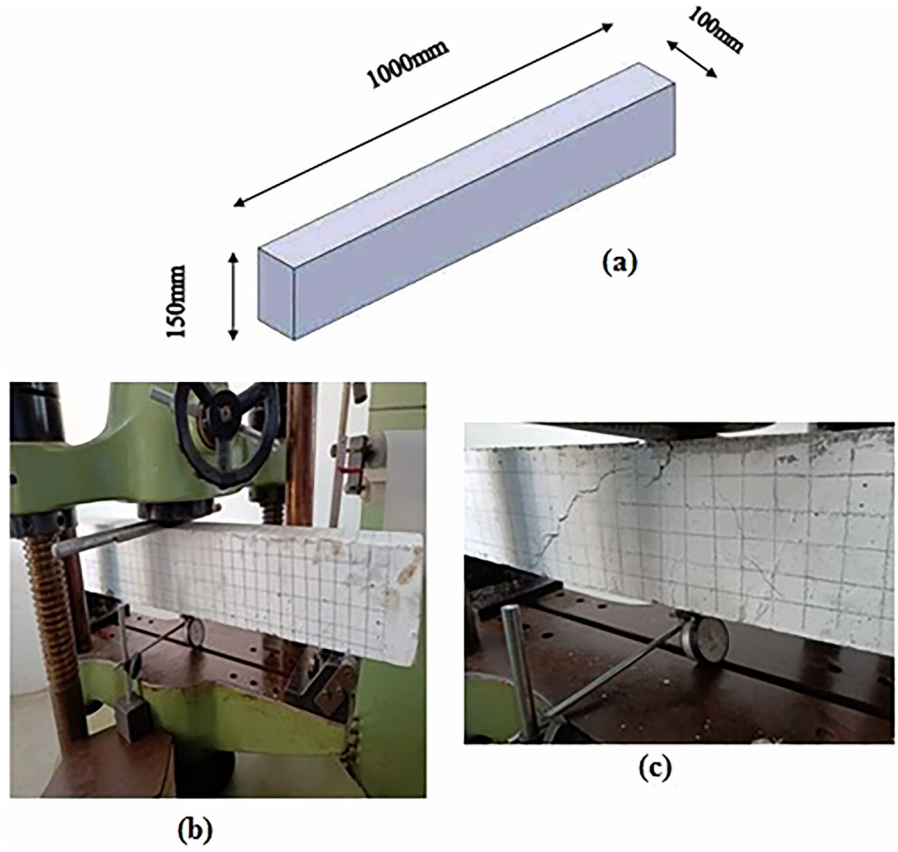


Figure 11: Three-point bending tests on notched specimens: **a.** geometrical details of beam, **b.** setup, **c.** cracked samples after the test.

The superior performance of NRB mixes can be directly linked to microstructural refinements observed in SEM analysis. Specifically, in NRB4, nano-additives effectively filled voids, enhanced packing density, and reinforced the interfacial transition zone. This modification forced cracks to branch and deviate around fibres and densified regions rather than propagating in a straight path. The additional crack deflection consumed more energy, thereby accounting for the higher fracture toughness. This behaviour was consistent with the superior mechanical strengths of NRB4, including compressive strength (53.45 MPa), split tensile strength (5.62 MPa), flexural strength (5.62 MPa), and modulus of elasticity (38.45 GPa). In addition to high mechanical and fracture performance, the best-performing mixes, particularly NRB4, also displayed satisfactory workability, with slump values within the practical range (99 mm). This ensured ease of placement and proper compaction without compromising strength. Although detailed durability studies were not conducted, the combination of increased modulus of elasticity and reduced crack propagation in NRB4 suggests a higher resistance to long-term degradation. Furthermore, the incorporation of waste-derived materials such as RHA and nMSWIA promotes sustainability by reducing the demand for cement and lowering the environmental footprint of the concrete.

Overall, the remarkable fracture energy improvements observed in RB and NRB mixes are not only numerical outcomes but also directly supported by microstructural evidence. The synergistic effect of fibre bridging under repeated loading and matrix densification through nano-additives explains the superior energy absorption capacity, toughness, and durability. These combined benefits establish NRB4 as the most reliable and sustainable blend, offering balanced workability, mechanical strength, and enhanced structural performance.

4.7. Mathematical analysis

The deflection analysis in beams is crucial for ensuring various engineering applications' structural integrity and serviceability. High-strength beams offer significant advantages in weight reduction and improved load-carrying capacity due to their material properties. However, their inherent stiffness can lead to serviceability concerns, particularly excessive deflection under operational loads. The necessitates accurate methods for predicting and controlling beam deflection.

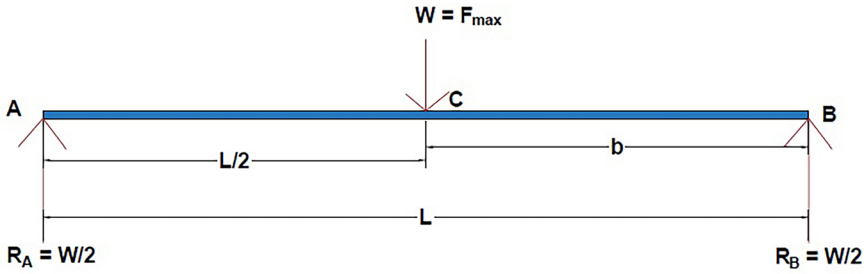


Figure 12: Supported beam model subjected to a point load.

This paper presents the application of the double integration method for analyzing the deflection of high-strength beams. This well-established technique leverages the relationship between the bending moment distribution and the curvature of the deflected beam. Through a series of integrations, the method allows for the determination of the slope and, ultimately, the deflection at any point along the beam's length. Figure 12 depicts a supported beam subjected to a point load (W) at its midpoint (L/2). The beam is labelled with points A, B, and C.

The deflection Y_c of a beam is related to the bending moment M_x through the flexural rigidity EI (where E is the modulus of elasticity and I is the moment of inertia (MoI) of the beam's cross-section). Equation 1 represents the bending moment equation. Equations 2 and 3 represent the slope and deflection of the high-strength concrete beam with basalt fibre.

$$M_x = R_B x - \mathrm{W(x-b)} \tag{1}$$

$$EI\frac{dy}{dx} = R_B\frac{x^2}{2} + C_1 + \frac{W(x-b)^2}{6} \tag{2}$$

$$EI.\mathrm{Y} = R_B\frac{x^3}{6} + C_1 x + C_1 - \frac{W(x-b)^3}{6} \tag{3}$$

By employing the given boundary conditions, determine the specific values of C1 and C2. Substitute X = L/2 and dy/dx = 0 into Equation 2 and solve for C1. To provide the value of the constant associated with the slope equation. Substitute X = 0 and y = 0 into Eq. Three and solve for C2. The yield value of the constant is associated with the deflection equation. With the obtained values of C1 and C2, Equation 3 (the deflection equation) allows us to calculate the deflection (Y) at any point along the beam's length (x) by substituting the specific values of x, EI, and the determined constants (C1 and C2) into Equation 3, its solve for the deflection (Y) at that particular point. This process can be repeated for various x values along the beam's length to obtain a complete deflection profile. Calculate the deflection at any desired point by substituting the corresponding x value into Equation 3 with the previously determined constants (C1 and C2).

Test results for HSRCB deflection agree well with mathematical predictions using the double integration method (Table 6). The average deflection of HSRCBs is 0.97. The standard deviation is 0.022, indicating a slight variation in deflection values. The coefficient of variation is 2.84, a unit less measure relative to the mean (0.97) and suggests a coefficient of variation around 3%.

An important aspect to consider when analyzing the deflection of the HSRCBs with basalt fibre reinforcement is the influence of material properties. While all the beam specimens have the exact dimensions (100 mm width and 150 mm depth), resulting in the exact moment of inertia, the critical factor causing deflection variation lies in the differing modulus of elasticity values across the mixes. This modulus, which signifies the material's stiffness, varies between beams based on their specific mix composition, ultimately influencing their load-carrying capacity.

Despite these variations in the modulus of elasticity, the comparison between the calculated and measured deflections reveals a reassuring closeness for all concrete mixes (Table 6). This encouraging observation suggests that when equipped with accurate material properties (including the mix-specific modulus of elasticity)

Table 6: Deflection value by double integration method.

SPECIMEN ID	MoE (E) (10^3 N/mm^2)	MoI (I) (10^6 mm^4)	MATHEMATICAL DEFLECTION (Y_c) (mm)	EXPERIMENTAL DEFLECTION (mm)	RATIO = EXP. / MATH. DEFLECTION
CC	28.65	28.12	2.62	2.50	0.95
MB1	29.35	28.12	3.75	3.70	0.98
NMB1	32.15	28.12	5.22	5.10	0.97
RB4	35.62	28.12	5.30	5.24	0.98
NRB4	38.45	28.12	7.15	7.10	0.99
Mean					0.97
SD					0.022
COV					2.84

and appropriate boundary conditions, the double integration method is a reliable tool for estimating deflection in HSRCBs with basalt fibre reinforcement.

4.8. Mode of failure

The HSRCB specimens continue to exhibit failure under single-point loading, as illustrated in Figure 13. The experimental investigation reveals that concrete crushing is the predominant mode of failure in all beams. Control beams experienced failures due to concrete crushing, flexural behaviour, and shear failure. Similarly, the failure mode of the specimens is typically divided into three stages: initially, a linear load-deflection response up to the beams' yield point, followed by elastic to plastic deformation where minor cracks propagate throughout the specimens, ultimately leading to failure upon reaching the ultimate load. Table 7 provides details on ductility and stiffness for all specimens.

In the modified beams, the presence of nano-additives and basalt fibres altered the crack patterns significantly. In MB1 and NMB1 specimens, multiple flexural cracks developed along the span instead of a few

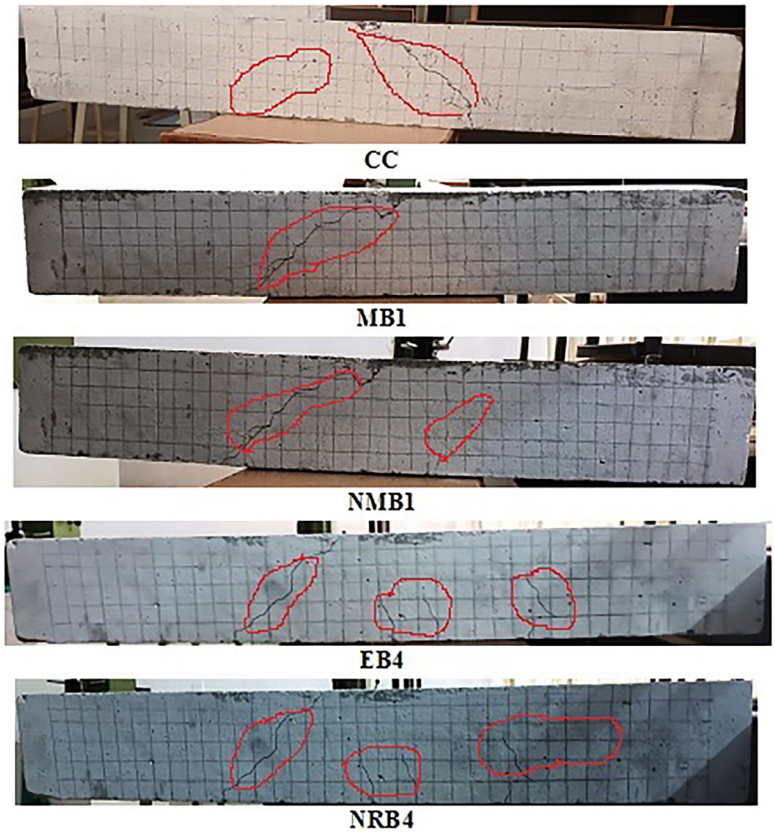


Figure 13: Failure mode of HSRCBs.

dominant cracks. These cracks were finer and more closely spaced, which delayed the onset of crushing in the compression zone. The EB4 specimen exhibited distributed cracking with smaller crack widths, indicating improved stress redistribution across the section. The NRB4 beam demonstrated the most desirable failure characteristics. Multiple microcracks formed gradually along the span, and their controlled propagation reduced stress concentration at a single point. The fibres effectively bridged cracks, restricting their opening and contributing to higher ductility and toughness. Crushing occurred only after significant deflection, showing that the beam was able to sustain higher loads with greater energy absorption.

Overall, the failure process of all beams could be divided into three stages: (i) an initial linear load–deflection response up to yielding, with no visible cracks; (ii) transition from elastic to plastic behaviour with gradual crack initiation and propagation; and (iii) the ultimate stage marked by widening of cracks, fibre pull-out (in fibre-reinforced specimens), and crushing of the concrete in the compression zone. The inclusion of waste-derived nano-additives and fibres not only reduced the severity of cracks but also enhanced ductility and stiffness, as summarised in Table 7.

The relationships between compressive strength and other mechanical properties demonstrate the consistent influence of basalt fibres and nano-additives (Figure 14). For compressive–tensile strength, most results lie

Table 7: Ultimate load, deflection, ductility and stiffness of the HSRCB.

SPECIMEN ID	BASALT FIBRE CONTENT (%)	ULTIMATE LOAD (KN)	YIELD DEFLECTION (MM)	ULTIMATE DEFLECTION (MM)	DUCTILITY	STIFFNESS (KN/MM)	MODE OF FAILURE
CC	0	6.55	2.36	2.50	1.06	5.95	CC + SF + FF
MB1	0.5	6.65	2.34	3.70	1.58	1.79	CC + FF
NMB1	0.5	7.96	2.15	5.10	2.37	1.56	CC + SF + FF
RB4	0.5	10.26	1.95	5.24	2.68	1.95	CC + SF
NRB4	0.5	12.65	1.80	7.10	3.94	1.78	CC + SF + FF

Note: SF-Shear failure; FF-Flexural failure; CC- Concrete crushing.

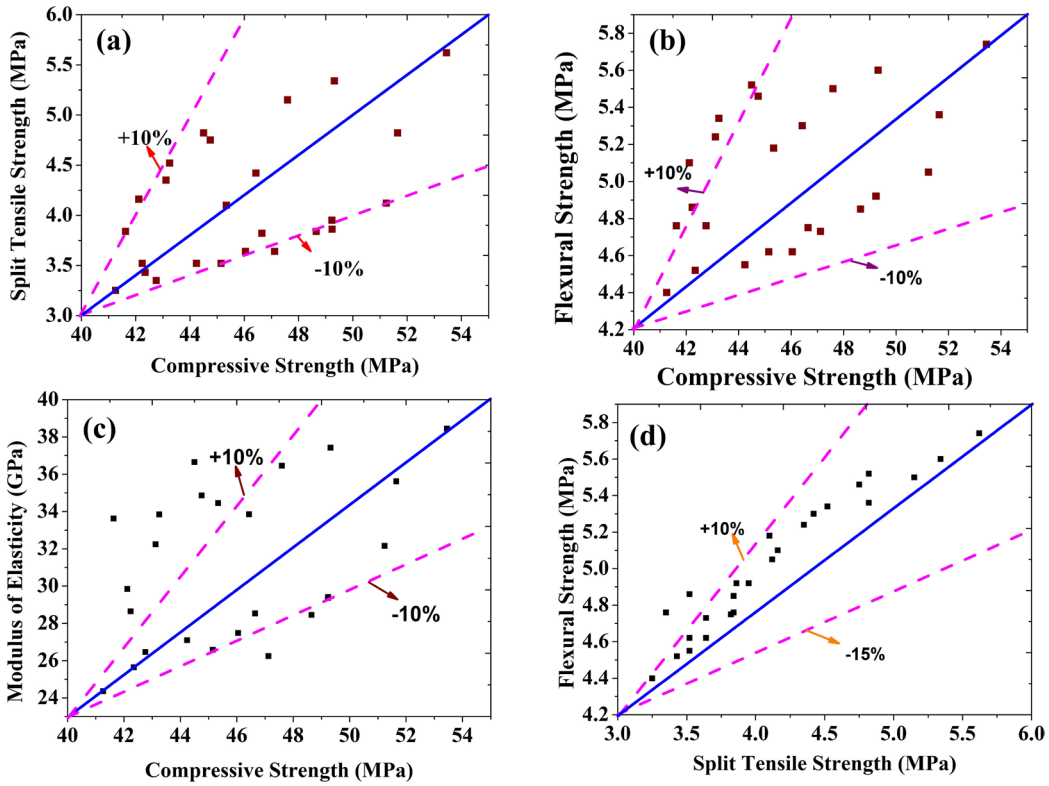


Figure 14: Relation between the mechanical properties of the HSRCBs.

within ±10% of the reference line, confirming proportionality between the two properties. A few mixes above the +10% limit reflect improved tensile behaviour due to fibre bridging, while those slightly below –10% indicate stronger gains in compressive strength, likely from localized densification or variable fibre dispersion. In the compressive–flexural relationship, most points lie above the reference line, showing that fibre reinforcement enhanced flexural performance beyond expected levels. This effect is particularly evident in mixes near or above +10%, where crack bridging and improved stress transfer played a significant role.

For compressive strength versus modulus of elasticity, most data scatter around the reference line, though several mixes exceeded the +10% boundary, indicating improved stiffness from pore refinement and a denser matrix. Some points closer to –10% suggest that stiffness did not always scale with compressive strength, possibly due to uneven fibre distribution. The flexural–tensile relationship further confirms the benefits of fibres and nano-additives, with most points within or above +10%, indicating higher flexural performance relative to tensile strength. Only a few results near –15% suggest premature cracking or reduced fibre efficiency. Overall, compressive–flexural and flexural–tensile correlations showed the strongest improvements, underscoring the role of fibre bridging and nano-modifications in enhancing flexural and tensile resistance.

5. CONCLUSION AND FUTURE STUDIES

The study aimed to investigate the influence of incorporating various types of ashes, like MSWIA, nMSWIA, RHA, and nRHA, along with basalt fibre, on the mechanical properties and performance of HSRCB. The experimental results and analyses yielded several significant conclusions:

- Among the various mixes tested, the NRB4 mix (containing nRHA and basalt fibre) exhibited the most promising results. It demonstrated superior load capacity, deflection control, ductility, and stiffness, making it an ideal candidate for high-strength concrete applications.
- Incorporating nano-additives and basalt fibre significantly enhanced the mechanical properties of the concrete. The NRB4 mix showed the highest ultimate load capacity (12.65 kN) and ultimate deflection (7.10 mm), indicating improved structural integrity and flexibility. The ductility and stiffness values for NRB4 were also higher than other mixes, further highlighting its robustness.
- The study confirmed that the modulus of elasticity, which varies with the specific mix composition, plays a crucial role in the deflection behaviour of HSRCBs. The close correlation between calculated and measured deflections suggests that predictive models can reliably estimate beam performance with accurate material property inputs.
- The predominant failure mode observed across all tested beams was concrete crushing, coupled with flexural and shear failures. This indicates that while the beams were generally able to carry substantial loads, improvements in mix composition could further mitigate such failure modes.
- Utilizing waste materials like MSWIA, nMSWIA, RHA, and nRHA in concrete enhances the material properties and promotes sustainable construction practices by recycling industrial and agricultural waste. Adding basalt fibre further enhances these benefits by improving the mechanical performance of the concrete.

6. ACKNOWLEDGMENTS

The authors wish to acknowledge Department of Civil Engineering, Vivekanandha College of Technology for Women, Tiruchengode, Tamilnadu for the facility and support extended for the research work.

7. BIBLIOGRAPHY

[1] SUJITHA, V.S., RAMESH, B., XAVIER, R.J., "Effects of nano-materials on mechanical properties in cementitious construction materials for high-strength concrete applications: a review", *Journal of Adhesion Science and Technology*, v. 38, n. 20, pp. 3737–3768, May2024. doi: http://doi.org/10.1080/01694243.2024.2354093.

[2] ALKAYEM, N.F., SHEN, L., MAYYA, A., *et al.*, "Prediction of concrete and FRC properties at high temperature using machine and deep learning: A review of recent advances and future perspectives", *Journal of Building Engineering*, v. 83, pp. 108369, Dec. 2023.

[3] LIU, B., JIANG, Y., ZHANG, W., *et al.*, "Enhancing performance and sustainability: CRB600H high-strength reinforcement in recycled concrete", *Sustainable Materials and Technologies.*, v. 39, pp. e00788, Apr. 2024. doi: http://doi.org/10.1016/j.susmat.2023.e00788.

[4] KAŹMIEROWSKI, M., JASKULSKI, R., DRZAZGA, M., *et al.*, "Effects of the addition of short straight steel fibres on the strength and strains of high-strength concrete during compression", *Scientific Reports*, v. 14, n. 1, pp. 6989, Mar. 2024. doi: http://doi.org/10.1038/s41598-024-57574-1. PubMed PMID: 38523144.

[5] ZHOU, S., LUO, H., FENG, B., *et al.*, "Research on using municipal solid waste incineration bottom ash for cement-stabilized macadam", *Construction & Building Materials*, v. 425, pp. 135850, Apr. 2024. doi: http://doi.org/10.1016/j.conbuildmat.2024.135850.

[6] LU, J., YANG, X., LAI, Y., *et al.*, "Utilization of municipal solid waste incinerator bottom ash (MSWIBA) in concrete as partial replacement of fine aggregate", *Construction & Building Materials*, v. 414, pp. 134918, Feb. 2024. doi: http://doi.org/10.1016/j.conbuildmat.2024.134918.

[7] LATHA, A.T., MURUGESAN, B., KABEER, K.S., "Valorization of municipal solid waste incinerator bottom ash for the production of compressed stabilized earth blocks", *Construction & Building Materials*, v. 423, pp. 135827, Apr. 2024. doi: http://doi.org/10.1016/j.conbuildmat.2024.135827.

[8] WĘGLIŃSKI, S., MARTYSZ, G., "Utilization of municipal solid waste incineration bottom ash in cement-bound mixtures", *Sustainability*, v. 16, n. 5, pp. 1865, Feb. 2024. doi: http://doi.org/10.3390/su16051865.

[9] LIU, J., WU, Y., CHENG, L., *et al.*, "Recycling of municipal solid waste incineration bottom ash (MSWIBA) particles into natural fine sands for sustainable engineering cementitious composites", *Construction & Building Materials*, v. 418, pp. 135500, Mar. 2024. doi: http://doi.org/10.1016/j.conbuildmat.2024.135500.

[10] CHEN, B., YE, G., "The role of water-treated municipal solid waste incineration (MSWI) bottom ash in microstructure formation and strength development of blended cement pastes", *Cement and Concrete Research*, v. 178, pp. 107440, Apr. 2024. doi: http://doi.org/10.1016/j.cemconres.2024.107440.

[11] DENG, J., WU, G., XIA, Y., *et al.*, "Preparation and hydration properties of sodium silicate-activated municipal solid waste incineration bottom ash composite ground-granulated blast furnace slag cementitious materials", *Materials*, v. 17, n. 10, pp. 2406, May. 2024. doi: http://doi.org/10.3390/ma17102406. PubMed PMID: 38793472.

[12] KHATIB, J., JAHAMI, A., EL KORDI, A., *et al.*, "Effect of municipal solid waste incineration bottom ash (MSWI-BA) on the structural performance of reinforced concrete (RC) beams", *Journal of Engineering, Design and Technology*, v. 21, n. 3, pp. 862–882, May. 2023. doi: http://doi.org/10.1108/JEDT-01-2021-0068.

[13] LU, J., YANG, X., LAI, Y., *et al.*, "Utilization of municipal solid waste incinerator bottom ash (MSWIBA) in concrete as partial replacement of fine aggregate", *Construction & Building Materials*, v. 414, pp. 134918, Feb. 2024. doi: http://doi.org/10.1016/j.conbuildmat.2024.134918.

[14] WĘGLIŃSKI, S., MARTYSZ, G., "Utilization of municipal solid waste incineration bottom ash in cement-bound mixtures", *Sustainability*, v. 16, n. 5, pp. 1865, Feb. 2024. doi: http://doi.org/10.3390/su16051865.

[15] DURGALAKSHMI, S., ILANGO, T., SINGH, A.P., *et al.*, "Study on the application of processed municipal solid waste ash for sustainable construction materials", *E3S Web of Conferences*, v. 399, pp. 03017, 2023.

[16] HAMCUMPAI, K., NUAKLONG, P., CHINDASIRIPHAN, P., *et al.*, "High-strength steel fibre-reinforced geopolymer concrete utilizing recycled granite waste and rice husk ash", *Construction & Building Materials*, v. 433, pp. 136693, Jun. 2024. doi: http://doi.org/10.1016/j.conbuildmat.2024.136693.

[17] KASHEM, A., KARIM, R., DAS, P., *et al.*, "Compressive strength prediction of sustainable concrete incorporating rice husk ash (RHA) using hybrid machine learning algorithms and parametric analyses", *Case Studies in Construction Materials*, v. 20, pp. e03030, Jul. 2024. doi: http://doi.org/10.1016/j.cscm.2024.e03030.

[18] LIU, F., JIN, B., HE, Q., *et al.*, "Influence of rice husk ash on the mechanical properties of ultra-high strength engineered cementitious composites (UHS-ECC)", *PLoS One*, v. 19, n. 4, pp. e0301927, Apr. 2024. doi: http://doi.org/10.1371/journal.pone.0301927. PubMed PMID: 38635748.

[19] HAMCUMPAI, K., NUAKLONG, P., CHINDASIRIPHAN, P., *et al.*, "High-strength steel fibre-reinforced geopolymer concrete utilizing recycled granite waste and rice husk ash", *Construction & Building Materials*, v. 433, pp. 136693, Jun. 2024. doi: http://doi.org/10.1016/j.conbuildmat.2024.136693.

[20] KASHEM, A., KARIM, R., DAS, P., *et al.*, "Compressive strength prediction of sustainable concrete incorporating rice husk ash (RHA) using hybrid machine learning algorithms and parametric analyses",

Case Studies in Construction Materials, v. 20, pp. e03030, Jul. 2024. doi: http://doi.org/10.1016/j.cscm.2024.e03030.

[21] MA, W., WANG, Y., HUANG, L., *et al.*, "Natural and recycled aggregate concrete containing rice husk ash as replacement of cement: mechanical properties, microstructure, strength model and statistical analysis", *Journal of Building Engineering*, v. 66, pp. 105917, May2023. doi: http://doi.org/10.1016/j.jobe.2023.105917.

[22] MUHAMMAD, J.H., YOUSIF, A.R., "Shear behavior of normal and high-strength concrete beams reinforced with BFRP bars and basalt macro fibres", *Construction & Building Materials*, v. 408, pp. 133516, Dec. 2023. doi: http://doi.org/10.1016/j.conbuildmat.2023.133516.

[23] MUHAMMAD, J.H., YOUSIF, A.R., "Effect of basalt minibars on the shear strength of BFRP-reinforced high-strength concrete beams", *Case Studies in Construction Materials*, v. 18, pp. e02020, Jul. 2023. doi: http://doi.org/10.1016/j.cscm.2023.e02020.

[24] TAHWIA, A.M., HELAL, K.A., YOUSSF, O., "Chopped basalt fibre-reinforced high-performance concrete: an experimental and analytical study", *Journal of Composites Science*, v. 7, n. 6, pp. 250, Jun. 2023. doi: http://doi.org/10.3390/jcs7060250.

[25] VATIN, N.I., HEMATIBAHAR, M., GEBRE, T.H., "Impact of basalt fibre reinforced concrete in protected buildings: a review", *Frontiers in Built Environment*, v. 10, pp. 1407327, May. 2024. doi: http://doi.org/10.3389/fbuil.2024.1407327.

[26] LI, S., SUN, Y., QIAN, Y., *et al.*, "Flexural behaviour of post-tensioned precast beams manufactured with basalt-fibre-reinforced recycled concrete–conventional concrete", *Journal of Building Engineering*, v. 89, pp. 109154, Jul. 2024. doi: http://doi.org/10.1016/j.jobe.2024.109154.

[27] XU, X., JIANG, Z., WAN, M., *et al.*, "Experimental study on performance of reinforced concrete short columns repaired and strengthened with Basalt fibre ultra-high-performance concrete (BF-UHPC)", *Structures*, v. 62, pp. 106170, 2024. doi: http://doi.org/10.1016/j.istruc.2024.106170.

[28] SHOAIB, S., EL-MAADDAWY, T., EL-HASSAN, H., *et al.*, "Numerical analysis of shear critical BFRP-reinforced concrete beams containing basalt fibres", *Structures*, v. 63, pp. 106442, 2024. doi: http://doi.org/10.1016/j.istruc.2024.106442.

[29] SUN, J., HE, D., SHEN, Z., *et al.*, "Experimental study on durability of steel-basalt fibre reinforced concrete under multiple factors coupling", *Construction & Building Materials*, v. 426, pp. 136090, May. 2024. doi: http://doi.org/10.1016/j.conbuildmat.2024.136090.

[30] ABDALLA, J.A., HAWILEH, R.A., BAHURUDEEN, A., *et al.*, "A comprehensive review on the use of natural fibres in cement/geopolymer concrete: a step towards sustainability", *Case Studies in Construction Materials*, v. 19, pp. e02244, 2023. doi: http://doi.org/10.1016/j.cscm.2023.e02244.

[31] AYYADURAI, A., MARUTHAI, S.M., MUTHU, D., "Impact of fly ash and banana fibre on mechanical performance of paver block concrete", *Gradevinar*, v. 76, n. 3, pp. 211–222, 2024. doi: http://doi.org/10.14256/JCE.3873.2023.

[32] JAHAMI, A., DAYAA, L., ASSAAD, J.J., *et al.*, "Flexural strength of structural beams cast using combined normal-weight and lightweight concrete mixtures", *Buildings.*, v. 14, n. 12, pp. 3787, Nov. 2024. doi: http://doi.org/10.3390/buildings14123787.

[33] KHATIB, J., JAHAMI, A., EL KORDI, A., *et al.*, "Effect of municipal solid waste incineration bottom ash (MSWI-BA) on the structural performance of reinforced concrete (RC) beams", *Journal of Engineering, Design and Technology*, v. 21, n. 3, pp. 862–882, May2023. doi: http://doi.org/10.1108/JEDT-01-2021-0068.

[34] JAHAMI, A., ZEAITER, N., CHEAIB, M., "Reviewing the potential: a comprehensive review of natural fibers (NFs) in structural concrete and their multifaceted influences", *Innovative Infrastructure Solutions*, v. 9, n. 4, pp. 102, Apr. 2024. doi: http://doi.org/10.1007/s41062-024-01384-x.

[35] KATAKAM, R., GOBINATH, R., SHYAMALA, G., "Research trend and knowledge gap analysis on fracture energy based concrete analysis and design", *Journal of Infrastructure Preservation and Resilience*, v. 6, n. 1, pp. 1–6, Dec. 2025. doi: http://doi.org/10.1186/s43065-025-00129-z.

[36] NASSAR, A.K., KATHIRVEL, P., MURALI, G., "Fracture behaviour of sustainable activators-based fibrous alkali-activated concrete under mode I, I/III & III loading", *Structural Engineering and Mechanics*, v. 93, n. 4, pp. 247, Jan. 2025.

[37] MURALI, G., NASSAR, A.K., KATHIRVEL, P., *et al.*, "Harnessing waste for sustainable construction: a novel synthesizing activators from waste for one-part geopolymer concrete and evaluating its fracture toughness", *Theoretical and Applied Fracture Mechanics*, v. 134, pp. 104745, Dec. 2024. doi: http://doi.org/10.1016/j.tafmec.2024.104745.

[38] ALAA, M., MAKHLOUF, M.H., MANSOUR, M.H., *et al.*, "Flexural behavior of reactive powder concrete ferrocement hollow beams reinforced by different mesh type", *International Journal of Concrete Structures and Materials*, v. 19, n. 1, pp. 1–9, Dec. 2025. doi: http://doi.org/10.1186/s40069-025-00772-6.

[39] KATHIRVEL, P., KALIYAPERUMAL, S.R., "Influence of recycled concrete aggregates on the flexural properties of reinforced alkali activated slag concrete", *Construction & Building Materials*, v. 102, pp. 51–58, Jan. 2016. doi: http://doi.org/10.1016/j.conbuildmat.2015.10.148.

[40] KE, S., GAO, Z., "Experimental and numerical study on flexural behavior of steel fiber reinforced high–strength concrete (SFRHC) beams", *Scientific Reports*, v. 15, n. 1, pp. 18338, May2025. doi: http://doi.org/10.1038/s41598-025-02220-7. PubMed PMID: 40419544.

[41] SHAO, J., JIANG, H., ZHANG, L., *et al.*, "Experimental study on flexural behavior of bonded steel-concrete composite beams", *Scientific Reports*, v. 15, n. 1, pp. 11451, Apr. 2025. doi: http://doi.org/10.1038/s41598-025-94906-1. PubMed PMID: 40181019.

[42] JUMAA, N.H., ALI, I.M., NASR, M.S., *et al.*, "Strength and microstructural properties of binary and ternary blends in fly ash-based geopolymer concrete", *Case Studies in Construction Materials*, v. 17, pp. e01317, Dec. 2022. doi: http://doi.org/10.1016/j.cscm.2022.e01317.

[43] KIM, K., SHIN, M., CHA, S., "Combined effects of recycled aggregate and fly ash towards concrete sustainability", *Construction & Building Materials*, v. 48, pp. 499–507, Nov. 2013. doi: http://doi.org/10.1016/j.conbuildmat.2013.07.014.

[44] KOCAK, Y., NAS, S., "The effect of using fly ash on the strength and hydration characteristics of blended cements", *Construction & Building Materials*, v. 73, pp. 25–32, Dec. 2014. doi: http://doi.org/10.1016/j.conbuildmat.2014.09.048.

[45] MAHOUTIAN, M., LUBELL, A.S., BINDIGANAVILE, V.S., "Effect of powdered activated carbon on the air void characteristics of concrete containing fly ash", *Construction & Building Materials*, v. 80, pp. 84–91, Apr. 2015. doi: http://doi.org/10.1016/j.conbuildmat.2015.01.019.

[46] NADEEM, A., MEMON, S.A., LO, T.Y., "The performance of fly ash and metakaolin concrete at elevated temperatures", *Construction & Building Materials*, v. 62, pp. 67–76, Jul. 2014. doi: http://doi.org/10.1016/j.conbuildmat.2014.02.073.

[47] AYYADURAI, A., SARAVANAN, M.M., DEVI, M., "Efficient wastewater treatment through integrated water hyacinth systems: advances and applications in concrete", *Materials Technology*, v. 58, n. 2, pp. 173–184, Apr. 2024.

[48] AYYADURAI, A., SARAVANAN, M.M., DEVI, M., "Performance of self compacting concrete using marble cutting slurry waste and silica fume", *Journal of University of Shanghai for Science and Technology.*, v. 23, n. 10, pp. 673–686, Oct. 2021.